Molecular Simulation of α-Olefins Using a New United-Atom Potential Model: Vapor−Liquid Equilibria of Pure Compounds and Mixtures

Theodora Spyriouni,[†,‡] Ioannis G. Economou,*[,†] and Doros N. Theodorou[†,‡]

Contribution from the Molecular Modelling of Materials Laboratory, Institute of Physical Chemistry, National Research Centre for Physical Sciences "Demokritos", GR 15310 Aghia Paraskevi Attikis, Greece, and Department of Chemical Engineering, University of Patras, GR 26500 Patras, Greece

Received July 13, 1998. Revised Manuscript Received January 19, 1999

Abstract: A new united atom potential model was developed for the vapor−liquid phase equilibrium of α-olefins ranging from 1-butene to 1-octene. The vapor pressure, normal boiling point, second virial coefficient, heat of vaporization, and structure were calculated with the new model, over a wide temperature range, and compared to experimental data. Critical constants of pure components were reproduced satisfactorily. Furthermore, this model was used to calculate the 1-butene−*n*-hexatriacontane and 1-hexene−*n*-hexatriacontane mixture phase equilibria at high pressure. Pressure-composition phase diagrams and lower critical solution temperature curves were constructed and compared to limited literature experimental data and predictions from an equation of state.

Introduction

The development of novel processes and products in the chemical, petrochemical and polymer industries over the past few years has increased the use of α-olefins as reactants, intermediates, or end products. Consequently, the accurate knowledge of the thermodynamic properties and phase equilibria of systems (pure components or multicomponent mixtures) containing α-olefins is vital for the optimal design of such processes and products.

Molecular simulation provides a valuable tool for such calculations, given a suitable molecular model for the various components. Several molecular models proposed over the past decade can be used, in principle, for the simulation of α-olefins. However, most of these models (such as CHARMM,[1] AMBER,[2] MMFF94,[3] and OPLS-AA[4]) were developed in order to reproduce best structural properties and energetic properties (heat of vaporization etc.) of the pure components at ambient conditions and so they are not expected to be accurate for phase equilibria.[5] Furthermore, these models are all-atom models (they account for the hydrogens explicitly), and some of them account for the vibrational degrees of freedom with enormous computational time requirements. A previous united-atom model relevant to the systems studied here is that of Jorgensen and co-workers,[6] where a model for 1-butene was proposed and tested for several thermodynamic properties (liquid density, heat of vaporization, boiling point, thermal expansion coefficient, and compressibility) and conformational properties, at 25 °C only. The absence of an appropriate molecular model for the description of the phase equilibrium properties of α-olefins and their mixtures over a wide temperature range was, consequently, one of the motivations for this work.

Phase equilibrium calculations of systems containing small molecules are conducted either in the Gibbs ensemble[7] or the Grand Canonical ensemble,[8] where molecule exchanges between the phases under consideration are feasible. The need to deal with long-chain molecules led to the invention of alternative techniques that attempt to overcome difficulties associated with the molecular size. Such an attempt includes the combination of the Gibbs ensemble with configurational bias[9] techniques in order to facilitate insertions or deletions of chain molecules.[10,11] Mehta and Kofke[12] used an iterative scheme for the phase equilibria of pure fluids and mixtures, based on the Gibbs−Duhem integration technique along the binodal curve. More recently, Mehta and Kofke[13] proposed a pseudo-grand canonical ensemble where molecule exchanges are replaced with volume fluctuations. Camp and Allen,[14] extended this idea to a pseudo-

* To whom correspondence should be addressed. E-mail: economou@mistras.nrcps.ariadne-t.gr.

† National Research Center for Physical Sciences "Demokritos".

‡ University of Patras.

(1) Smith, J. C.; Karplus, M. *J. Am. Chem. Soc.* **1992**, *114*, 801−812.

(2) Cornell, W. D.; Cieplak, P.; Bayly, C. I.; Gould, I. R.; Merz, K. M., Jr.; Ferguson, D. M.; Spellmeyer, D. C.; Fox, T.; Caldwell, J. W.; Kollman, P. A. *J. Am. Chem. Soc.* **1995**, *117*, 5179−5197.

(3) Halgren, T. A. *J. Comput. Chem.* **1996**, *17*, 490−615.

(4) Jorgensen, W. L.; Maxwell, D. S.; Tirado-Rives, J. *J. Am. Chem. Soc.* **1996**, *118*, 11225−11236.

(5) Chen, B.; Martin, M. G.; Siepmann, J. I. *J. Phys. Chem. B* **1998**, *102*, 2578−2586.

(6) Jorgensen, W. L.; Madura, J. D.; Swenson, C. J. *J. Am. Chem. Soc.* **1984**, *106*, 6638−6646.

(7) Panagiotopoulos, A. Z. *Mol. Phys.* **1987**, *61*, 813−826.

(8) Frenkel, D.; Smit. B. *Understanding Molecular Simulation*; Academic Press: New York, 1996.

(9) (a) Siepmann, J. I.; Frenkel, D. *Mol. Phys.* **1992**, *75*, 59−70. (b) Frenkel, D.; Mooij, G. C. A.; Smit, B. *J. Phys.: Condens. Matter* **1992**, *4*, 3053−3076. (c) de Pablo, J. J.; Laso, M.; Suter, U. W. *J. Chem. Phys.* **1992**, *96*, 2395−2403.

(10) Siepmann, J. I.; Karaborni, S.; Smit, B. *Nature* **1993**, *365*, 330−332.

(11) Martin, M. G.; Siepmann, J. I. *J. Phys. Chem.* **1998**, *102*, 2569−2577.

(12) (a) Mehta, M.; Kofke, D. A. *Chem. Eng. Sci.* **1994**, *49(16)*, 2633−2645. (b) Kofke, D. A. *Mol. Phys.* **1993**, *78(6)*, 1331−1336.

(13) Mehta, M.; Kofke, D. A. *Mol. Phys.* **1995**, *86(1)*, 139−147.

(14) Camp, P. J.; Allen, M. P. *Mol. Phys.* **1996**, *88(6)*, 1459−1469.

10.1021/ja982453y CCC: $18.00
Published on Web 03/24/1999

Table 1. Atomistic Molecular Model for α-Olefins

description	potential function and parameters
nonbonded interactions	$U_{LJ}(r_{ij}) = 4\epsilon[(\sigma_{ij}/r_{ij})^{12} - (\sigma_{ij}/r_{ij})^{6}]$
	$\epsilon(CH_3)/k_B = \epsilon(CH_2)/k_B = 47.66$ K; $\sigma(CH_3) = \sigma(CH_2) = \sigma(CH(sp^2)) = 3.915$ Å
	$\epsilon(CH(sp^2))/k_B = 81.69$ K; $\sigma(CH_2(sp^2)) = 3.905$ Å
	$\epsilon(CH_2(sp^2))/k_B = 89.93$ K
bond lengths	Fixed values
	$C(sp^3) - C(sp^3) = C(sp^3) - C(sp^2) = 1.53$ Å
	$C(sp^2) - C(sp^2) = 1.331$ Å
bond angles	Fixed values
	$C - C(sp^3) - C = 112°$
	$C - C(sp^2) - C = 124°$
dihedral angles	$U_{tors}(\phi)/k_B = c_0 + c_1(1 + \cos\phi) + c_2(1 - \cos(2\phi)) + c_3(1 + \cos(3\phi))$
	C−C−C−C: $c_0 = 0$ K, $c_1 = 355.03$ K
	$c_2 = -68.19$ K, $c_3 = 791.32$ K
	C−C−C=C: $c_0 = 685.96$ K, $c_1 = 86.31$ K,
	$c_2 = -109.71$ K, $c_3 = 282.08$ K

Gibbs ensemble in order to simulate the two phases in parallel. Both schemes require the evaluation of the chemical potential and the pressure at each density sampled by the system. Escobedo and de Pablo[15] presented a variation of the pseudo-Gibbs ensemble method in which volume fluctuations are suppressed in favor of particle exchanges. They also proposed an expanded Gibbs ensemble scheme where the difference from conventional Gibbs ensemble is that insertions or deletions of a chain molecule are performed gradually, by "segmental" exchanges.[16] This ensemble has been used by de Pablo and co-workers for the phase equilibrium simulation of pure *n*-alkanes[17] and their mixtures.[18] Finally, a new iterative Monte Carlo scheme was introduced for the simulation of phase equilibria of chain systems (SPECS)[19] and was applied to binary mixture phase equilibria of different size components. In SPECS, insertions, deletions, or exchanges of long chain molecules between phases are avoided, and equilibrium is reached only through the variation of the number of solvent molecules in each phase. In essence, SPECS is a pseudo-ensemble scheme[13,20] that allows efficient location of phase boundaries. The chemical potential of long chain molecules is calculated from the segmental chemical potential using the Chain Increment Ansatz.[21,22] Recently, Escobedo[20] reviewed different pseudo-ensemble schemes for the simulation of multicomponent phase equilibria.

In this work, an optimized united-atom molecular model is proposed for simulating the thermodynamic properties and vapor−liquid equilibrium (VLE) of α-olefins ranging from 1-butene to 1-octene, over a wide temperature range approaching the pure component critical point. The pure components were simulated in the Gibbs ensemble. Coexisting vapor and liquid densities, vapor pressures, second virial coefficients, heats of vaporization, and structural properties were calculated and compared with experimental data. Furthermore, high-pressure phase equilibrium calculations were conducted for mixtures containing a long hydrocarbon (*n*-hexatriacontane, *n*-C_{36}) and an α-olefin (1-butene or 1-hexene), using the SPECS algorithm. Pressure-composition phase diagrams and lower critical solution temperature (LCST) curves were constructed and compared against limited experimental data available and predictions from an equation of state (statistical-associating-fluid theory, SAFT)[23] that is expected to be accurate for such types of mixtures.

Potential Model Development

The first target of this work was to capture the VLE properties of pure α-olefins of intermediate size (1-butene up to 1-octene) over a wide temperature range, with the same molecular model. Previous work by Jorgensen et. al[6] resulted in a group contribution transferable united-atom potential model (OPLS). The OPLS model was optimized for liquid densities, heats of vaporization, boiling points, and structural properties for several short linear and branched alkanes and 1-butene, at 25 °C. Preliminary phase equilibrium calculations for 1-butene with OPLS resulted in considerable deviations from experiment, especially at high temperatures, and unsatisfactory estimates of the critical constants.

The molecular model developed in this work is a united-atom model, where the nonbonded intra- and intermolecular interactions are calculated with a Lennard−Jones (LJ) potential. The potential parameter optimization was carried out with the constraint of keeping the bond lengths and the bond angles (which are considered constant) close to their experimental values. The parameter values for the new model are shown in Table 1. The optimization of the LJ energy (ϵ) and size (σ) parameters was carried out by assuming three types of interaction sites, namely, an alkane site and two sites on each side of the double bond. The initial values for the LJ parameters of the alkane part ($\epsilon/k_B = 49.32$ K, $\sigma = 3.94$ Å) were from the Dodd and Theodorou potential.[24] This potential was initially used for calculating the bulk liquid density and structure of long chain linear alkanes up to *n*-C_{78},[24] and also the chemical potential[22] and vapor−liquid equilibrium[25] of linear alkanes up to *n*-C_{16}. The sites around the double bond were initially attributed higher ϵ values to account for the more polarizable nature of the electron cloud around the double bond. The σ values were the same for all sites, except for the outer site next to the double bond, for which it was found that a smaller size resulted in better fitting of the VLE properties.

The final set of parameters shown in Table 1 was attained using a scaling methodology based on the corresponding states

(15) Escobedo, F. A.; de Pablo, J. J. *J. Chem. Phys.* **1997**, *106*, 2911−2923.
(16) Escobedo, F. A.; de Pablo, J. J.; *J. Chem. Phys.* **1996**, *105*, 4391−4394.
(17) Nath, S.; Escobedo, F. A.; de Pablo, J. J. *J. Chem. Phys.* **1998**, *108*, 9905−9911.
(18) Nath, S.; Escobedo, F. A.; de Pablo, J. J.; Patramai, I. *Ind. Eng. Chem. Res.* **1998**, *37*, 3195−3202.
(19) Spyriouni, T.; Economou, I. G.; Theodorou, D. N. *Phys. Rev. Lett.* **1998**, *80(20)*, 4466−4469.
(20) Escobedo, F. A. *J. Chem. Phys.* **1998**, *108*, 8761−8772.
(21) Kumar, S. K.; Szleifer, I.; Panagiotopoulos, A. Z. *Phys. Rev. Lett.* **1991**, *66*, 2935−2938.
(22) Spyriouni, T.; Economou, I. G.; Theodorou, D. N. *Macromolecules* **1997**, *30*, 4744−4755.
(23) Chapman, W. G.; Gubbins, K. E.; Jackson, G.; Radosz, M. *Ind. Eng. Chem. Res.* **1990**, *29*, 1709−1721.
(24) Dodd, L. R.; Theodorou, D. N. *Adv. Pol. Sci.* **1994**, *116*, 249−281.
(25) Spyriouni, T.; Economou, I. G.; Theodorou, D. N. *Macromolecules* **1998**, *31*, 1430−1431.

principle.[26] However, as the bond lengths scale with the σ parameter, several initial sets of ϵ and σ parameters were tried to keep the bond lengths close to their experimental values (1.54 Å for the single bond and 1.34 Å for the double bond). Admittedly, this is a simplified two-body model that accounts implicitly for the many body effects, mainly due to the double bond. Furthermore, the model does not distinguish between methyl and methylene groups. The large difference in polarizability and dipole moment between C═C and C−C bonds may result in optimum values for the olefin methyl and methylene parameters which do not coincide with the corresponding best parameters for paraffins. In other words, the LJ parameter values obtained should be seen, to a large extent, as adjustable parameters, their values depending on the data set used to optimize them.

The torsional potential dictating the internal rotations was taken from Jorgensen et. al.[6] Rotations around all single bonds not sharing a carbon atom with the double bond are described by a standard potential with three minima, appropriate for alkanes. Rotations around the single bond adjacent to the double bond are described by the same type of potential, using different sets of Fourier coefficients. The syn conformation is taken as $\phi = 0°$ for all calculations. The dihedral angle distribution for the first (alkane-type) torsional potential exhibits a global maximum in the trans ($\phi = 180°$) and local maxima in the gauche+ ($\phi = 60°$) and gauche− ($\phi = -60°$) conformations. For the second torsional potential, the maximum population is observed in the skew+ ($\phi = 120°$) and skew− ($\phi = -120°$) conformations, and there is a local maximum of population in the syn conformation ($\phi = 0°$).

The Dodd and Theodorou potential[24] was used for the simulation of the long hydrocarbon (*n*-C_{36}). This potential treats the methyl and methylene groups with the same energetic and size parameters ($\epsilon/k_B = 49.32$ K, $\sigma = 3.94$ Å). The torsional potential of Ryckaert and Bellemans, which is very similar to the Jorgensen et. al[6] torsional potential for *n*-alkanes, was used, while the bond lengths and bond angles were kept fixed (l = 1.54 Å, $\theta = 112°$). This potential has given very accurate phase equilibrium predictions for mixtures of heavy hydrocarbons with ethane or with ethylene.[19]

Simulation Details

Pure Components. Pure 1-butene, 1-hexene, and 1-octene were simulated in the NVT Gibbs ensemble. The moves employed in the course of a Gibbs simulation were displacements of the molecules in each phase, volume fluctuations, and exchanges of molecules between phases. In addition, for molecules larger than 1-butene, a cut and regrowth process was used for segments after the third, similar to the configurational bias (CB) move.[9] The number of molecules of 1-butene, 1-hexene, and 1-octene in the systems studied was 150, 120, and 100, respectively. To ensure that the system size was sufficient for the thermodynamic properties under consideration, several state points of 1-octene were simulated with 200 molecules. Equilibrium averages were collected over about 1×10^7 steps, and the relative number of displacements (including CB type of moves), volume fluctuations, and exchanges of molecules was 40−70%, 1%, and 30−60%, respectively. Block averaging with 10 blocks was used to calculate statistical uncertainty. For all runs, the pair potential was truncated at $r = 2.3\sigma$, and tail corrections were taken into account by direct integration.[27] A quintic spline was used between $r = 1.45\sigma$ and $r = 2.3\sigma$ to eliminate discontinuities associated with the truncation.[28]

Mixtures. In the present work, binary mixtures of *n*-C_{36} with 1-butene and 1-hexene were studied. The pressure-composition phase diagram of 1-butene-*n*-C_{36} at $T = 442.6$ K and $T = 473$ K, and the LCST curve at $P = 50$ bar were calculated. The LCST curve for the 1-hexene-*n*-C_{36} mixture at P=20 bar was also constructed.

The binary mixture phase equilibrium simulations were conducted using the SPECS algorithm developed previously[19] and thus, here only a brief introduction to the algorithm is given. In SPECS, one phase (phase I) rich in light solvent (component 1), and a second phase (phase II) rich in heavy hydrocarbon (component 2), are simulated in parallel in the f_1N_2PT ensemble, under common values of f_1, P, and T. In each phase, the set fugacity f_1 of component 1 is attained via insertions and deletions of light solvent molecules according to the following acceptance criteria:

$$p_{\text{ins}} = \min\left(1, \frac{\rho_{\text{new}}}{\rho_{\text{old}}}\right) = \min\left[1, \frac{J_{1,\text{ins}}\beta f_1 V \exp(-\beta\Delta U)}{(N_1+1)Z_1^{\text{intra}}}\right]$$

$$p_{\text{del}} = \min\left(1, \frac{\rho_{\text{new}}}{\rho_{\text{old}}}\right) = \min\left[1, \frac{N_1 Z_1^{\text{intra}} \exp(-\beta\Delta U)}{J_{1,\text{del}}\beta f_1 V}\right] \quad (1)$$

$J_{1,\text{ins}}$ and $J_{1,\text{del}}$ are the Jacobians of transformation from Cartesian to generalized coordinates for the inserted and the deleted molecule of component 1, respectively, and are equal to $\sin\psi \prod_{j=1}^{n_1-2} \sin\theta_j$, where ψ is the polar angle defining the orientation of the first bond, θ_j is the jth bond angle, and n_1 is the number of interaction sites per molecule. ΔU is the energy change brought about by the insertion or the deletion of a solvent molecule, V is the volume of the system, N_1 is the number of molecules of component 1, and $\beta = 1/(k_BT)$, where k_B is the Boltzmann constant. Z_1^{intra} is the configurational integral of the inserted or deleted molecule in the ideal gas phase:

$$Z_1^{\text{intra}} = 8\pi^2 \int \prod_{j=1}^{n_1-2} \sin\theta_j \, d\theta_1 ... d\theta_{n_1-2} \, d\phi_2 ... d\phi_{n_1-2} \times \exp[-\beta U_1^{\text{intra}}(\theta_1, ...\theta_{n_1-2}, \phi_2, ..., \phi_{n_1-2})] \quad (2)$$

where ϕ are the dihedral angles and U_1^{intra} is the total intramolecular energy of the molecule.

The two phases reach equilibrium when the fugacities of component 2 in each phase are equal, since the fugacities of component 1 are set to be equal and the two phases are simulated under the same T and P. The heavy hydrocarbon chemical potential calculations were greatly facilitated by invoking the chain increment Ansatz,[21] according to which the chemical potential of a long chain molecule is a linear function of its length beyond a minimum length. It has been shown[22] that this Ansatz is very realistic for linear hydrocarbons and the minimum length of the chain can be taken as six carbon atoms. The SPECS algorithm was designed to force the equilibrium requirement $f_2^{\text{I}} = f_2^{\text{II}}$ through a Newton−Raphson iteration scheme where the value of f_1 imposed on both phases is corrected by a value given by the following expression, derived from the Gibbs−Duhem equation:

$$\Delta \ln f_1 = x_2^{\text{I}} x_2^{\text{II}} \frac{\ln f_2^{\text{II}} - \ln f_2^{\text{I}}}{x_2^{\text{I}} - x_2^{\text{II}}} \quad (3)$$

where x_2 is the mole fraction of component 2. The iteration scheme proceeds until $\Delta \ln f_1$ is sufficiently small.

The moves employed in the mixture calculations in order to equilibrate the long hydrocarbon molecules were concerted rotation[29] (ConRot), which rearranges the internal conformation of a molecule, configuration bias[9] (CB), which cuts and regrows segments from the end of a chain molecule, and reptation, which cuts a segment from one end and appends it to the other end. The number of *n*-C_{36} chains was equal to 15 for all the systems studied. Each productive run

(26) Prausnitz, J. M.; Lichtenthaler, R. N.; Azevedo, A. G. *Molecular Thermodynamics of Fluid-Phase Equilibria*, 2nd ed.; Academic Press: New York, 1986.

(27) Allen, M. P.; Tildesley, D. J. *Computer Simulation of Liquids*; Oxford University Press: New York, 1987.

(28) Theodorou, D. N.; Suter, U. W. *Macromolecules* **1985**, *18*, 1467−1478.

Table 2. Critical Temperature (T_c), Pressure (P_c), Density (ρ_c) and Normal Boiling Point (T_b) of α-Olefins Experimental Data and Simulation Results from the New Model

	T_c (K)		P_c (bar)		ρ_c (g/cm^3)		T_b (K)	
alkene	expt[32]	simul.	expt[32]	simul.	expt[32]	simul.	expt[31]	simul.
1-butene	419.5_5	424_2	40.2_5	40_1	0.233_{12}	0.22_1	266.9	264
1-hexene	504.0_3	512_4	32.1_3	31_2	0.237_5	0.23_1	336.6	331
1-octene	567.0_8	581_7	26.8_8	27_2	0.24_1	0.23_1	394.4	394

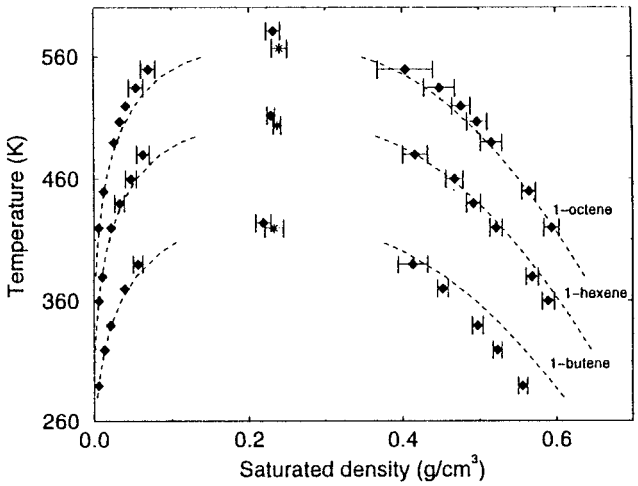

Figure 1. Vapor−liquid coexistence curves for 1-butene, 1-hexene, and 1-octene. Experimental coexistence data[30,31] (dashed lines), experimental critical points[32] (stars), simulated coexistence densities with the new model, and extrapolated critical points based on simulation at subcritical conditions (filled diamonds). Error bars are shown when greater than symbol size.

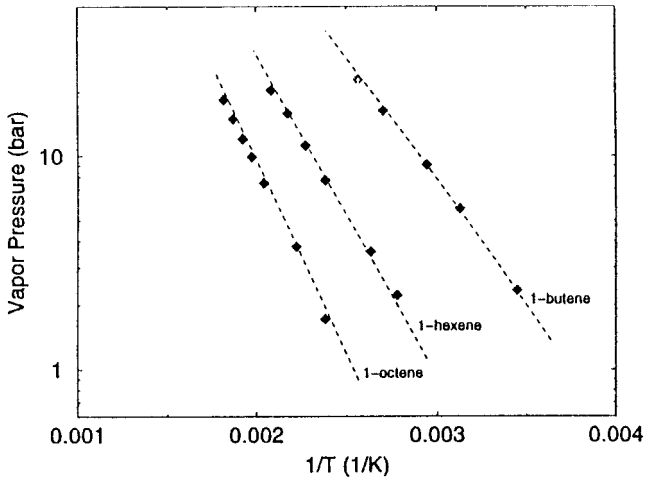

Figure 2. Vapor pressure as a function of the inverse temperature for 1-butene, 1-hexene, and 1-octene. Experimental data[30] (dashed lines) and simulation results (filled diamonds).

consisted of about 4×10^7 steps. The Lorentz−Berthelot combining rules[26] were used for the unlike pair interactions.

Results and Discussion

Pure Components. The vapor−liquid coexistence curves of the three α-olefins studied here are given in Figure 1 and in tabular form as Supporting Information.

The experimental saturated liquid densities are from the DIPPR data compilation of pure compound properties,[30] the experimental data for the vapor densities are from the Lee−Kesler correlation[31] and the experimental critical properties are taken from Tsonopoulos and Ambrose.[32] The critical properties T_c, and ρ_c (see Table 2) were estimated by fitting the simulated liquid and vapor densities to the rectilinear diameter rule and to the scaling relationship for the width of the coexistence curve

$$\frac{\rho_{liq} + \rho_{vap}}{2} = \rho_c + A(T - T_c) \quad (4)$$

$$\rho_{liq} - \rho_{vap} = B(T - T_c)^{\beta} \quad (5)$$

where β is the critical exponent, taken equal to an Ising-type critical exponent ($\beta = 0.32$).

The agreement between the experimental and the predicted saturated densities, in both vapor and liquid phases, is satisfactory for all the olefins studied here. The relatively higher deviation observed in the liquid density of 1-butene reveals the relative insufficiency of the new model at short chain lengths, which is expected to be more pronounced for even shorter olefins (propylene). Certainly, the accuracy of the model could be improved by distinguishing the methyl from the methylene group and/or modifying the single and double bond length values. However, the emphasis of this work was to show that a relatively simple molecular model performs well for the phase equilibria of pure α-olefins and, more importantly, for mixtures of α-olefins with heavy hydrocarbons, as will be discussed in the following paragraph.

The predicted critical temperatures (see Table 2) are slightly shifted to higher values compared to the experimental values (overestimation by 1.1% for 1-butene, 1.6% for 1-hexene, and 2.5% for 1-octene), while experimental and simulated critical density values agree within the experimental and statistical simulation error in all cases. In Table 2, the normal boiling point T_b of each α-olefin is also given, along with the experimental values.[31] The deviation is 1.1% for 1-butene, 1.7% for 1-hexene, and 0.1% for 1-octene.

Experimental data[30] and simulation results for the vapor pressure of the three α-olefins are shown in Figure 2. The agreement is excellent in all cases. The critical pressures P_c (see Table 2) were estimated from this graph by a simple linear extrapolation and were found to agree well with the experimental critical pressures.[32]

Simulation results for the coexisting densities and vapor pressure of 1-octene using 200 molecules are practically indistinguishable from the calculations with 100 molecules. The numerical details can be found in Tables S1, S2, and S3 of Supporting Information.

The second virial coefficient B was calculated according to the well-known expression

(29) (a) Pant, P. V. K.; Theodorou, D. N. *Macromolecules* **1995**, *28*, 7224−7234. (b) Dodd, L. R.; Boone, T. D.; Theodorou, D. N. *Mol. Phys.* **1993**, *78*, 961−996.

(30) DIPPR Data Compilation of Pure Compound Properties, Design Institute for Physical Properties Data, American Institute of Chemical Engineers, 1987.

(31) Reid, R. C.; Prausnitz, J. M.; Poling, B. E. *The Properties of Gases and Liquids*, 4th ed.; McGraw-Hill: New York, 1987.

(32) Tsonopoulos, C.; Ambrose, D. *J. Chem. Eng. Data* **1996**, *41*, 645−656.

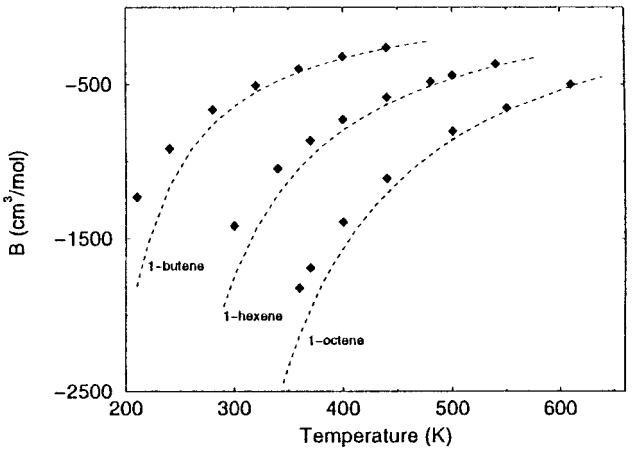

Figure 3. Second virial coefficient, B, of 1-butene, 1-hexene, and 1-octene. Experimental data[33] (dashed lines) and simulation results (filled diamonds).

$$B(T) = -2\pi\int[\langle\exp(-\beta U_{\text{inter}})\rangle_{\omega} - 1]r^2\,\mathrm{d}r \qquad (6)$$

where U_{inter} is the intermolecular energy between two chain molecules with a distance r between their centers of mass, and the subscript ω denotes averaging over all possible orientations and conformations of each molecule, sampled according to $\exp(-\beta U_{\text{intra}})$. Experimental data[33] and simulation results for the second virial coefficient are shown in Figure 3. The agreement is very satisfactory over a wide temperature range. Deviations from the experimental data are higher at low temperatures. At these conditions the experimental uncertainty is on the order of 100 cm^3/mol.[34]

The enthalpy of vaporization is calculated directly from the simulation data, using the expression

$$\Delta H_{\text{liq}\rightarrow\text{vap}} = U_{\text{vap}} - U_{\text{liq}} + P_{\text{sat}}\left(\frac{1}{\rho_{\text{vap}}} - \frac{1}{\rho_{\text{liq}}}\right) \qquad (7)$$

where U_{vap} (U_{liq}) is the total internal energy of the vapor (liquid) phase, P_{sat} is the saturated pressure, and ρ_{vap} (ρ_{liq}) is the molar density of the vapor (liquid) phase. In Figure 4, simulation results are compared against experimental data[30] for a wide temperature range. The agreement is quite satisfactory. As temperature approaches the critical value, deviations arise because of the small overprediction of the critical temperature by the model.

Intra- and intermolecular mer−mer distribution functions are shown in Figures 5a and 5c for 1-hexene (solid line) and *n*-hexane (dashed line) at $T = 400$ K and molar density $\rho = 0.007$ mol/cm^3. Calculations for *n*-hexane were performed using the Dodd and Theodorou potential for *n*-alkanes, and are shown for comparison. The first two peaks of the intramolecular pair density function $\omega(r)$, shown in Figure 5a, are at separation values equal to the double bond length (1.331 Å), and to the single bond length (1.53 Å for 1-hexene, 1.54 Å for *n*-hexane), respectively. Three sharp peaks appear for both molecules at approximately 2.53 Å (corresponding to the distance between three successive carbon atoms), 3.9 Å (corresponding to a trans conformation), and 5.08 Å (corresponding to two successive trans conformations). The corresponding peaks for *n*-hexane are slightly shifted to the right because of the longer single bond length. Other characteristic peaks for 1-hexene appear at approximately 2.87 Å (syn conformation), 3.03 Å (gauche conformation), 3.59 Å (skew conformation), 4.4 Å (syn−trans conformation), 4.9 Å (skew−trans conformation), and 5.25 Å (trans−trans−syn conformation). The pair density function for

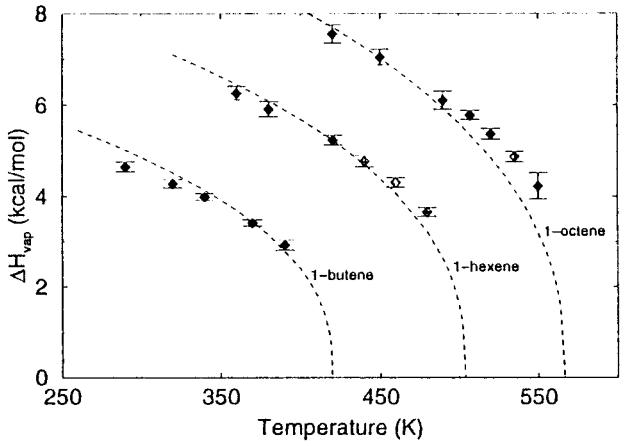

Figure 4. Enthalpy of vaporization of 1-butene, 1-hexene, and 1-octene. Experimental data (dashed lines) and simulation results (filled diamonds).

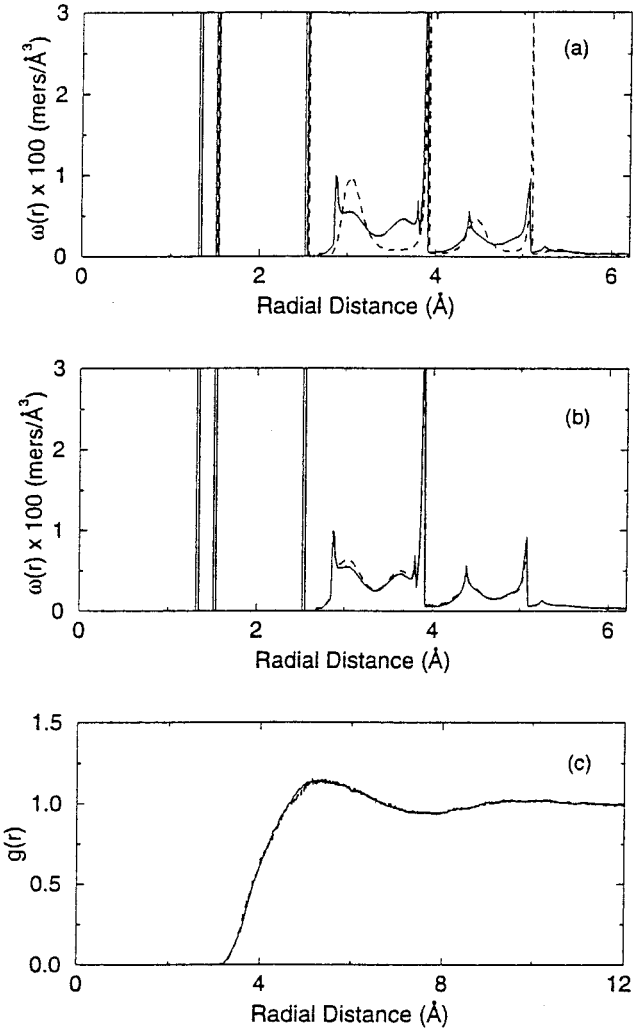

Figure 5. (a) Intramolecular pair density function $\omega(r)$ for 1-hexene (solid line) and *n*-hexane (dashed line) at $T = 400$ K and molar density $\rho = 0.007$ mol/cm^3. (b) $\omega(r)$ for 1-hexene in the bulk (solid line) and as a continuous unperturbed chain (dashed line), at $T = 400$ K. (c) Intermolecular distribution function $g(r)$ for 1-hexene (solid line) and *n*-hexane (dashed line) at the same conditions with (a).

(33) Tsonopoulos, C.; Heidman, J. L. *Fluid Phase Equilib.* **1990**, *57*, 261−276.

(34) Tsonopoulos, C.; Dymond, J. H.; Szafranski, A. M. *Pure Appl. Chem.* **1989**, *61(8)*, 1387−1394.

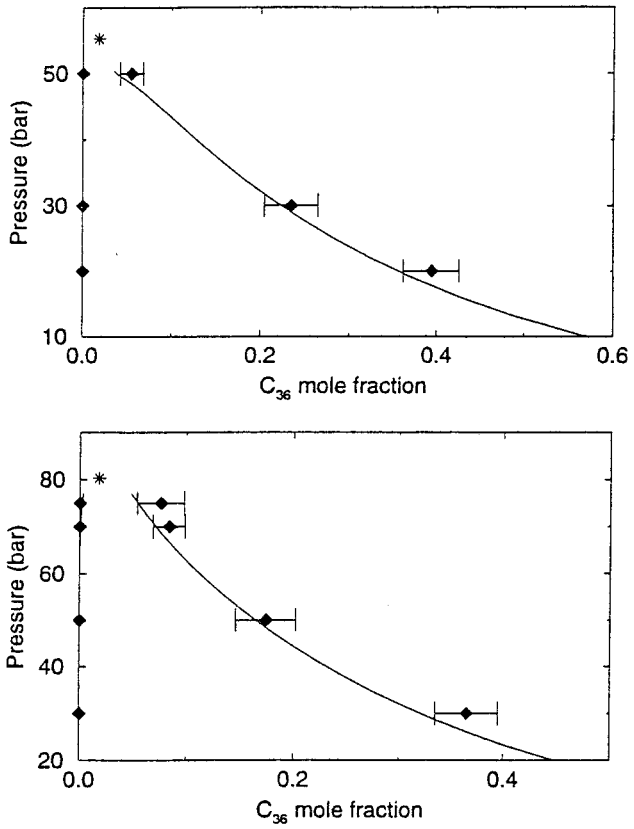

Figure 6. Pressure−composition phase diagram for the 1-butene−*n*-C_{36} mixture, at $T = 442.6$ K (top) and $T = 473$ K (bottom). Experimental data[37] (stars), simulation results (filled diamonds), and SAFT predictions (solid lines).

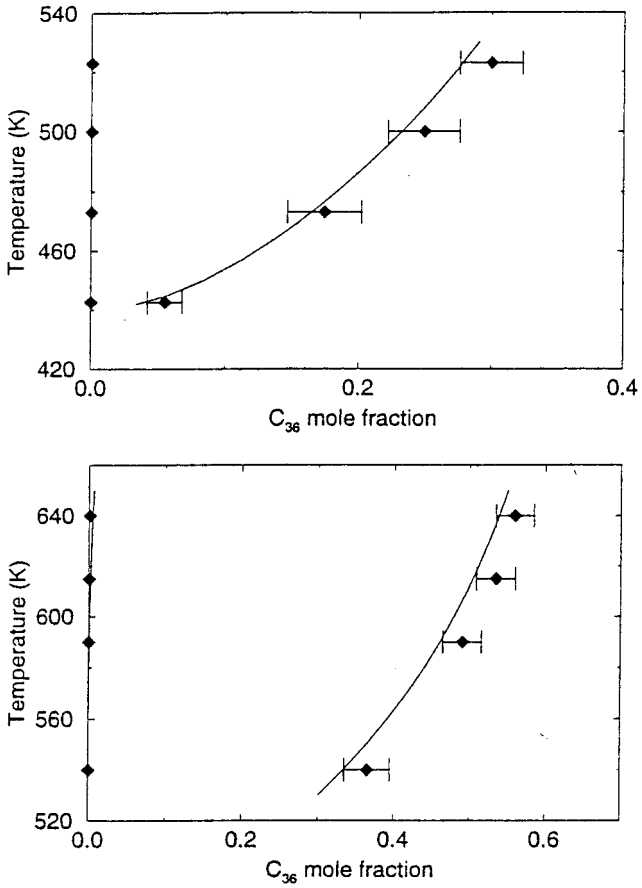

Figure 7. LCST curve for the 1-butene−*n*-C_{36} mixture at $P = 50$ bar (top), and the 1-hexene−*n*-C_{36} mixture at $P = 20$ bar (bottom). Simulation results (filled diamonds) and SAFT predictions (solid lines).

n-hexane exhibits also maxima at approximately: 3.05 Å (gauche conformation), 4.47 Å (trans−gauche conformation), and 5.4 Å (trans−trans−gauche conformation).

The intramolecular pair density function was also calculated for continuous unperturbed[35] 1-hexene (i.e., devoid of nonlocal interactions between mers separated by more than four bonds) at $T = 400$ K, and is shown in Figure 5b along with the same function in the bulk. The comparison is good, although not as perfect as seen in longer linear hydrocarbons.[22] This indicates that, to a good approximation, 1-hexene adopts conformations according to Flory's "random coil hypothesis".[35]

The intermolecular pair distribution function $g(r)$ is shown in Figure 5c. Results from 1-hexene and *n*-hexane are almost indistinguishable. The first coordination shell appears at a distance of approximately 5.1 Å, which is shorter than that observed for longer alkanes[22] (5.9 Å for *n*-C_{16}). This indicates that these short C_6 chains pack more tightly than longer chains, presumably because they are more rodlike.

Mixtures. Binary mixtures of long hydrocarbons with short α-olefins are very often encountered in the polymer (synthesis and processing) and petrochemical industries.[36] Therefore, the knowledge of their phase behavior is very important for numerous industrial applications. Unfortunately, experimental data are very limited, at least in the open literature, due to practical difficulties associated with such mixtures and so one has to rely to empirical correlations. An attractive alternative is molecular simulation using realistic models. In the present work, binary mixtures of 1-butene and 1-hexene with *n*-C_{36} were studied. Two isothermal pressure-composition diagrams (442.6 and 473 K) for 1-butene-*n*-C_{36} are plotted in Figure 6 and are consistent with the limited experimental data[37] available (shown with stars). Predictions from the SAFT equation of state,[23] which is widely used in industry and academia to model polymer systems, are shown for comparison. Although SAFT was shown[19,18] to be inaccurate for the phase equilibrium of highly asymmetric mixtures (such as ethylene-*n*-C_{40}), it is expected to become progressively better as the size of the solvent increases.[36] From the calculations presented here, one can conclude that molecular simulation and SAFT are in good agreement.

In Figure 7a and b, two LCST diagrams are shown, for the binary mixtures 1-butene-*n*-C_{36} at $P = 50$ bar and 1-hexene-*n*-C_{36} at $P = 20$ bar, respectively. The LCST type[26] of phase equilibrium is quite common for mixtures consisting of asymmetric components, in the vicinity of the solvent's critical point, and is mainly driven by large density differences between the solvent and the heavy hydrocarbon (free volume effects). Experimental data for these mixtures are not available for comparison. The simulation is in good agreement with SAFT predictions for both mixtures.

Conclusions

In this work, a new united-atom potential model was introduced that was optimized for the phase equilibrium of α-olefins ranging from 1-butene to 1-octene. The new model gives satisfactory predictions for saturated densities, vapor pressures, normal boiling points, second virial coefficients, and

(35) Flory, P. J. *Principles of Polymer Chemistry;* Cornell University Press: Ithaca, NY, 1953.

(36) Folie, B.; Radosz, M. *Ind. Eng. Chem. Res.* **1995**, *34*, 1501−1516 and references therein.

(37) Gregg, C. J.; Stein, F. P.; Chen, S.; Radosz, M. *Ind. Eng. Chem. Res.* **1993**, *32*, 1442−1448.

heats of vaporization for these α-olefins, over a wide temperature range, including the critical region. Binary mixture phase equilibrium calculations at high pressure were performed for 1-butene-*n*-C_{36} and 1-hexene-*n*-C_{36}, using the new potential. Two isothermal pressure-composition phase diagrams (442.6 and 473 K) and the LCST curve at 50 bar were calculated for the 1-butene-*n*-C_{36} mixture. In addition, the LCST curve at 20 bar was constructed for the 1-hexene-*n*-C_{36} mixture. Comparison with limited experimental data available revealed that computer simulation can perform well for mixture phase equilibrium calculations, given a suitable molecular model for the individual components. Although SAFT performs adequately for the mixtures examined here, it was shown to be inaccurate for other types of industrially important mixtures such as ethane and ethylene with heavy hydrocarbon,[18,19] and water with methane and with ethane.[38] In all these other cases, molecular simulation was shown to be in good agreement with the experimental data, providing, thus, a generally reliable predictive tool.

Supporting Information Available: Tables S1−S5 list the simulation results for the coexisting densities, vapor pressures, second virial coefficients, and enthalpies of vaporization of the α-olefins, and tables S6 and S7 list calculations for the binary mixtures (PDF). This material is available free of charge via the Internet at http://pubs.acs.org.

JA982453Y

(38) Errington, J. R.; Boulougouris, G. C.; Economou, I. G.; Panagiotopoulos, A. Z.; Theodorou, D. N. *J. Phys. Chem. B* **1998**, *102*, 8865−8873.